Journal of Solid State Chemistry 187 (2012) 211–218

Contents lists available at SciVerse ScienceDirect

Journal of Solid State Chemistry

journal homepage: www.elsevier.com/locate/jssc

# First-principles studies of Ni–Ta intermetallic compounds

Yi Zhou [a], Bin Wen [b,*], Yunqing Ma [a], Roderick Melnik [c,d], Xingjun Liu [a,**]

[a] Department of Materials Science and Engineering, College of Materials, and Research Center of Materials Design and Applications, Xiamen University, Xiamen 361005, China
[b] State Key Laboratory of Metastable Materials Science and Technology, Yanshan University, Qinhuangdao 066004, China
[c] M²NeT Lab, Wilfrid Laurier University, Waterloo,75 University Ave. West, Ontario, Canada N2L 3C5
[d] MIT Department, University of Jyväskylä, Jyväskylä, Finland

ARTICLE INFO

*Article history:*
Received 20 August 2011
Received in revised form
29 December 2011
Accepted 1 January 2012
Available online 10 January 2012

*Keywords:*
Intermetallics
Miscellaneous
Crystal chemistry of intermetallics
Ab-initio calculations

ABSTRACT

The structural properties, heats of formation, elastic properties, and electronic structures of Ni–Ta intermetallic compounds are investigated in detail based on density functional theory. Our results indicate that all Ni–Ta intermetallic compounds calculated here are mechanically stable except for P21/m-$Ni_3Ta$ and hc-$NiTa_2$. Furthermore, we found that Pmmn-$Ni_3Ta$ is the ground state stable phase of $Ni_3Ta$ polymorphs. The polycrystalline elastic modulus has been deduced by using the Voigt–Reuss–Hill approximation. All Ni–Ta intermetallic compounds in our study, except for NiTa, are ductile materials by corresponding $G/K$ values and poisson's ratio. The calculated heats of formation demonstrated that $Ni_2Ta$ are thermodynamically unstable. Our results also indicated that all Ni–Ta intermetallic compounds analyzed here are conductors. The density of state demonstrated the structure stability increases with the Ta concentration.



## 1. Introduction

Due to the high melting temperature, excellent properties in harsh environments, Ni–Ta alloys stand out as remarkable candidates for high-temperature materials [1], and they are highly attractive from scientific and technological points of view [2]. The first Ni–Ta phase diagram was published by Therkelsen [3] in 1933. After that, a substantial number of papers on Ni–Ta intermetallic phases has been published. Notably, in 1984, Nash et al. [4], pointed out that five intermetallic phases and two terminal solid solutions, FCC (Ni) and BCC (Ta) existing in Ni–Ta phases diagram. In 1991 and 1994, thermodynamic properties of this system were evaluated by adopting the CALPHAD approach by Kaufman [5] and Ansara et al. [6], respectively. In 1999, the Ni–Ta binary system was reassessed by Cui et al. [7] and a set of parameters describing the Gibbs energy of each phase was obtained through the CALPHAD method. In 2002, the phase equilibrium relationship and thermodynamic properties were analyzed by Pan et al. [1] by adopting the diffusion and EPMA methods. In 2009, the Gibbs free energy functions were evaluated and the associated equilibrium phase diagram was reported by Zhou et al. [8] by combining the CALPHAD method and first-principle calculations. Based on Ni–Ta phase diagrams studied by these researchers, it was revealed that five kinds of intermetallic compounds exist in the Ni–Ta system, namely, $Ni_8Ta$, $Ni_3Ta$, $Ni_2Ta$, NiTa, and $NiTa_2$.

Despite these efforts [8–10], there are a number of remaining long-standing questions about crystal structures and properties of Ni–Ta intermetallic compounds. For instance, it is known that $Ni_3Ta$ has three polymorphs (Pmmn-$Ni_3Ta$ with space group of Pmmn, I4/mmm-$Ni_3Ta$ with space group of I4/mmm and P21/m-$Ni_3Ta$ with space group of P21/m [4,8,11–16]) at different temperatures conditions. However, which polymorph is the ground stable phase is still a controversy. In addition, the mechanism of shape memory effect of $Ni_3Ta$ is still unclear. In order to uncover this mechanism, a study of intrinsic ductility and brittleness of $Ni_3Ta$ is needed. Furthermore, the crystal structures of $Ni_8Ta$ [4] and $NiTa_2$ [17,18] are undetermined to date, and a further study in this direction is required. Comprehensive studied on other properties of these alloys are lacking in the literatures, and composite dependent mechanical properties of Ni–Ta intermetallic compounds are missing. To fill in these gaps, in this work we undertake a systematical analysis of the structural, thermodynamic, mechanical, and electronic properties of the Ni–Ta intermetallic compounds by adopting first-principles calculations.

## 2. Computational method

In this work, five kinds of Ni–Ta intermetallic compounds and the corresponding eight crystal structures (namely, $Ni_8Ta$, I4/mmm-$Ni_3Ta$, Pmmn-$Ni_3Ta$, P21/m-$Ni_3Ta$, $Ni_2Ta$, NiTa, ha-$NiTa_2$ with ha Wyckoff atomic positions, and hc-$NiTa_2$ with hc Wyckoff

* Corresponding author.
** Corresponding author. Fax: +086 592 2183937.
*E-mail addresses:* wenbin@ysu.edu.cn (B. Wen), lxj@xmu.edu.cn (X. Liu).

0022-4596/$ - see front matter © 2012 Elsevier Inc. All rights reserved.
doi:10.1016/j.jssc.2012.01.001

atomic positions) have been considered. First-principles calculations have been performed by employing the CASTEP package [19], in which density functional theory (DFT) and the plane-wave pseudopotential technique are implemented. The ion–electron interaction is modeled by the ultrasoft pseudopotential method [20]. The generalized gradient approximation (GGA) [21] with the Perdew–Burke–Ernzerhof (PBE) [22] exchange-correlation functional has been used in the process of calculation. The kinetic cutoff energy for plane waves has been set as 400 eV [23]. The **k** point separation in the Brillouin zone of the reciprocal space is 0.07 $nm^{-1}$, that is, $4\times4\times5$ for I4/mmm-$Ni_3Ta$, $3\times3\times3$ for NiTa, $5\times5\times6$ for $Ni_2Ta$, $4\times4\times3$ for ha-$NiTa_2$, $4\times4\times3$ for hc-$NiTa_2$, $4\times4\times3$ for $Ni_8Ta$, and $3\times3\times3$ for Pmmn-$Ni_3Ta$, $3\times3\times2$ for P21/m-$Ni_3Ta$, respectively. A relationship between $Ni_2Ta$ primitive cell total energy and plane-wave cutoff energy was calculated to determine an appropriate cutoff energy for the plane-wave basis set. It is displayed obviously in Fig. 1 that the total energy changes little with the increasing of cutoff energy which exceeds 360 eV. Therefore, a cutoff energy of 400 eV is selected in this work.

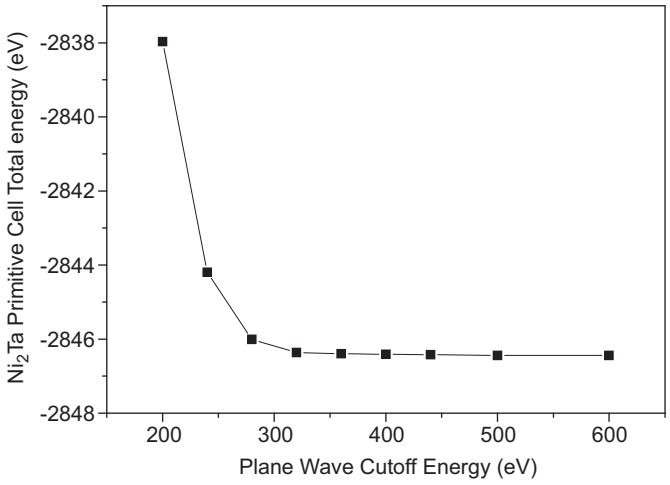


**Fig. 1.** The relationship between $Ni_2Ta$ primitive cell total energy and plane-wave cutoff energy.

Benchmark calculations have been performed for the $Ni_2Ta$ phase, pointing out that the computational scheme utilized in this work is credible. Indeed, the calculated lattice parameter of $a=0.3196$ nm, $c=0.8174$ nm compares well with the experimental value of $a=0.3160$ nm and $c=0.7950$ nm [24], $a=0.3154$ nm and $c=0.7905$ nm [25].

## 3. Results and discussion

### 3.1. Structural properties

By applying the experimental crystallographic data of the Ni–Ta intermetallic compounds from Refs. [4,8,11–18,24–35] as the original configurations, the lattice parameters and internal coordinates of the Ni–Ta intermetallic compounds have been optimized. The Convergence tolerance of energy, force, stress and displacement for Ni–Ta alloys are $1\times10^{-5}$ eV/atom, 0.03 eV/atom, 0.05 GPa and 0.001 Å, respectively. The calculated lattice parameters and the corresponding mass densities, together with the experimental [17–18,24–25,29–32,34–35] data, are shown in Table 1. As shown in Table 1, the lattice parameters and mass densities of all Ni–Ta intermetallic compounds agree perfectly with the corresponding experimental ones. This observation is an additional confirmation that the computational methodology adopted in this paper is suitable for the purpose of this study and the accuracy of our geometry optimizations is sufficient.

In Fig. 2, the calculated mass densities of Ni–Ta intermetallic compounds are plotted with corresponding existing experimental values. We observe that the mass density of Ni–Ta intermetallic compounds keeps a linear growth with Ta concentration $c$ (in at %). The relationship between the mass density (in $g/cm^3$) and the Ta concentration $c$ (in at %) can be described by the following formula: $\rho=9.38889+6.82437\ c$. As it is shown in Figure l, the calculated values of densities correspond satisfyingly with the experimental ones, which verifies the reliability of the calculation results.

**Table 1**
Theoretical lattice parameters and mass density compared to experimental values for the Ni–Ta intermetallic compounds.

| Compound | Space group | Mass density ($g/cm^3$) | Lattice parameters (nm) | Reference |
|---|---|---|---|---|
| Ni | Fm-3m | 8.842 | $a=0.3531$ | This work |
| | | 8.970 | $a=0.3515$ | [36] |
| | | 8.910 | $a=0.3524$ | [37] |
| | | | | [38] |
| $Ni_8Ta$ | I4/mmm | 10.061 | $a=0.7692$, $c=0.3623$ | This work |
| I4/mmm-$Ni_3Ta$ | I4/mmm | 11.422 | $a=0.3724$, $c=0.7527$ | This work |
| | | 12.090 | $a=0.3627$, $c=0.7455$ | [31] |
| Pmmn-$Ni_3Ta$ | Pmmn | 11.444 | $a=0.5181$, $b=0.4327$ $c=0.4622$ | This work |
| | | 12.130 | $a=0.5122$, $b=0.4522$ $c=0.4235$ | [32] |
| P21/m-$Ni_3Ta$ | P21/m | 11.383 | $a=0.4612$, $b=0.5209$ $c=0.8804$ | This work |
| | | 12.040 | $a=0.4532$, $b=0.5125$ $c=0.8632$ | [30] |
| $Ni_2Ta$ | I4/mmm | 11.870 | $a=0.3196$, $c=0.8174$ | This work |
| | | 12.480 | $a=0.3160$, $c=0.7950$ | [24] |
| | | 12.600 | $a=0.3154$, $c=0.7905$ | [25] |
| NiTa | R-3m | 13.168 | $a=0.4936$, $c=2.6834$ | This work |
| | | 13.750 | $a=0.4921$, $c=2.6905$ | [29] |
| ha-$NiTa_2$ | I4/mcm | 14.157 | $a=0.6355$, $c=0.4887$ | This work |
| | | 14.960 | $a=0.6197$, $c=0.4869$ | [17] |
| hc-$NiTa_2$ | I4/mcm | 13.532 | $a=0.6742$, $c=0.4542$ | This work |
| | | 14.840 | $a=0.6216$, $c=0.4872$ | [18] |
| Ta | Im-3m | 15.773 | $a=0.3365$ | This work |
| | | 16.630 | $a=0.3306$ | [39] |
| | | | | [40] |
| | | 16.670 | $a=0.3303$ | [41] |

### 3.2. Elastic properties and mechanical stability

In this work, the elastic constants $C_{ij}$ (GPa) and bulk modulus of the Ni–Ta intermetallic compounds have been evaluated, and the calculation results are summarized in Table 2. The mechanical stability of the Ni–Ta intermetallic compounds are studied through a mechanical stability criterion, known from the literature.

In particular, for monoclinic crystal, the conditions for mechanical stability are given by [42]:

$$C_{ij}>0(i=j,0<i\le 6),C_{33}C_{55}-C_{35}^2>0,C_{44}C_{66}-C_{46}^2>0,C_{22}C_{33}-C_{23}^2>0,$$
$$C_{11}+C_{22}C_{33}+2(C_{12}+C_{13}+C_{23})>0,$$
$$[C_{22}(C_{33}C_{55}-C_{35}^2)+2(C_{23}C_{25}C_{35}-C_{25}^2C_{55}-C_{25}^2C_{33})]>0,$$
$$\{2[C_{15}C_{25}(C_{33}C_{12}-C_{13}C_{23})+C_{15}C_{35}(C_{22}C_{13}-C_{12}C_{23})$$
$$+C_{25}C_{35}(C_{11}C_{23}-C_{12}C_{23})]-[C_{25}^2(C_{22}C_{33}-C_{23}^2)+C_{25}^2(C_{11}C_{33}-C_{23}^2)$$
$$+C_{35}^2(C_{11}C_{22}-C_{12}^2)]+C_{55}\}>0. \quad (1)$$

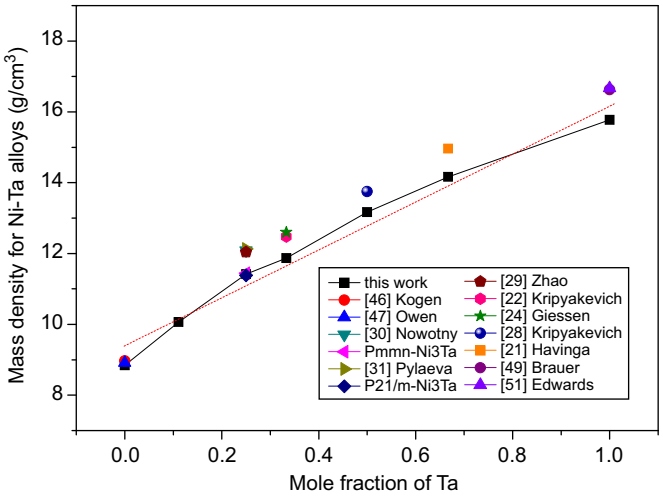


**Fig. 2.** Theoretical mass density compared to experimental values for the Ni–Ta intermetallic compounds.

In this study, the crystal structure of P21/m-$Ni_3Ta$ is monoclinic. According to the values from Table 2, the elastic constants of P21/m-$Ni_3Ta$ do not satisfy with the mechanical stability criteria given by (1), which confirms that P21/m-$Ni_3Ta$ is mechanical unstable.

The mechanical stability criteria for tetragonal structures can be expressed as follows [43]:

$$C_{11}>0,C_{33}>0,C_{44}>0,C_{66}>0,C_{11}-C_{12}>0,$$
$$C_{11}+C_{33}-2C_{13}>0,2C_{11}+C_{33}+2C_{12}+4C_{13}>0. \quad (2)$$

In this work, five Ni–Ta intermetallic compound crystal structures ($Ni_8Ta$, I4/mmm-$Ni_3Ta$, $Ni_2Ta$, ha-$NiTa_2$ and hc-$NiTa_2$) are tetragonal crystals. For $Ni_8Ta$, I4/mmm-$Ni_3Ta$, $Ni_2Ta$ and ha-$NiTa_2$, the elastic constants satisfy all stability criteria given by (2), which implies that these alloys are mechanically stable. However, for the hc-$NiTa_2$ structure, the elastic constants do not fulfill the restriction of $C_{11}>0$, $C_{44}>0$, $C_{11}-C_{12}>0$ and $C_{11}+C_{33}-2C_{13}>0$. This indicates that the hc-$NiTa_2$ structure is a mechanically unstable structure, and it cannot exist at temperature of 0 K.

Next, the mechanical stability criteria for orthorhombic structures can be given by the following inequalities [44]:

$$C_{ij}>0(i=j,0<i\le 6),C_{11}+C_{22}-2C_{12}>0,C_{11}+C_{33}-2C_{13}>0,$$
$$C_{22}+C_{33}-2C_{23}>0,C_{11}+C_{22}+C_{33}+2C_{12}+2C_{13}+2C_{23}>0. \quad (3)$$

As shown in Table 2, the elastic constants for orthorhombic Pmmn-$Ni_3Ta$ satisfy all stability criteria given by (3), and this implies that Pmmn-$Ni_3Ta$ is mechanically stable.

Finally, the mechanical stability conditions for hexagonal structures can be expressed as follows [45,46]:

$$C_{11}>0,\ C_{44}>0,\ C_{11}-C_{12}>0,\ (C_{11}+C_{12})\,C_{33}-2C_{13}^2>0. \quad (4)$$

For hexagonal NiTa considered in this paper, all values of elastic constants obey the mechanical stability conditions given by (4), which implies that the NiTa compound is mechanically stable.

**Table 2**
Calculated elastic properties for the single crystalline Ni–Ta intermetallic compounds.

| Compound | Elastic properties |
|---|---|
| $Ni_8Ta$ | $C_{11}=305$, $C_{12}=139$, $C_{13}=186$, $C_{16}=0$, $C_{33}=259$, $C_{44}=117$, $C_{66}=54$, $K=210$ |
| I4/mmm-$Ni_3Ta$ | $C_{11}=281$, $C_{12}=202$, $C_{13}=167$, $C_{16}=0$, $C_{33}=353$, $C_{44}=112$, $C_{66}=157$, $K=220$ |
| Pmmn-$Ni_3Ta$ | $C_{11}=388$, $C_{12}=109$, $C_{13}=144$, $C_{23}=148$, $C_{22}=376$, $C_{33}=367$, $C_{44}=81$, $C_{55}=102$, $C_{66}=70$, $K=215$ |
| P21/m-$Ni_3Ta$ | $C_{11}=364$, $C_{12}=141$, $C_{13}=148$, $C_{15}=7$, $C_{23}=125$, $C_{25}=-14$, $C_{35}=14$, $C_{46}=-18$, $C_{22}=384$, $C_{33}=350$, $C_{44}=69$, $C_{55}=80$, $C_{66}=83$, $K=214$ |
| $Ni_2Ta$ | $C_{11}=253$, $C_{12}=214$, $C_{13}=158$, $C_{16}=0$, $C_{33}=356$, $C_{44}=86$, $C_{66}=144$, $K=212$ |
| NiTa | $C_{11}=363$, $C_{12}=151$, $C_{13}=130$, $C_{33}=388$, $C_{44}=113$, $K=215$ |
| ha-$NiTa_2$ | $C_{11}=395$, $C_{12}=173$, $C_{13}=131$, $C_{16}=0$, $C_{33}=394$, $C_{44}=16$, $C_{66}=74$, $K=204$ |
| hc-$NiTa_2$ | $C_{11}=-565$, $C_{12}=979$, $C_{13}=226$, $C_{16}=0$, $C_{33}=315$, $C_{44}=-77$, $C_{66}=74$, $K=202$ |

$C_{ij}$, elastic constants (in GPa); $K$, bulk modulus (in GPa).

**Table 3**
Polycrystalline bulk modulus, shear modulus, Young's modulus (GPa), Poisson's ratios and valence electron densities (electron/Å$^3$) for mechanically stable Ni–Ta intermetallic compounds according to Voigt–Reuss–Hill approximation. $K$ is the bulk modulus (in GPa); $G$ is the shear modulus (in GPa); $E$ is Young's modulus (in GPa); $v$ is Poisson's ratio.

| Compound | $K_V$ | $K_R$ | $K_H$ | $G_V$ | $G_R$ | $G_H$ | $E$ | $G/K$ | $v$ | Valence electron density |
|---|---|---|---|---|---|---|---|---|---|---|
| $Ni_8Ta$ | 210 | 210 | 210 | 81 | 66 | 74 | 199 | 0.35 | 0.3424 | 0.193 |
| I4/mmm-$Ni_3Ta$ | 221 | 220 | 220 | 101 | 82 | 92 | 242 | 0.42 | 0.3174 | 0.224 |
| Pmmn-$Ni_3Ta$ | 215 | 215 | 215 | 99 | 94 | 96 | 252 | 0.45 | 0.3042 | 0.212 |
| $Ni_2Ta$ | 213 | 212 | 213 | 85 | 54 | 70 | 189 | 0.33 | 0.3526 | 0.227 |
| NiTa | 215 | 215 | 215 | 113 | 112 | 113 | 288 | 0.53 | 0.2765 | 0.242 |
| ha-$NiTa_2$ | 206 | 205 | 205 | 58 | 31 | 44 | 144 | 0.21 | 0.3945 | 0.256 |

Based on the above analysis, we conclude that, except for P21/m-$Ni_3Ta$ and hc-$NiTa_2$, all other Ni–Ta intermetallic compounds considered here are mechanically stable.

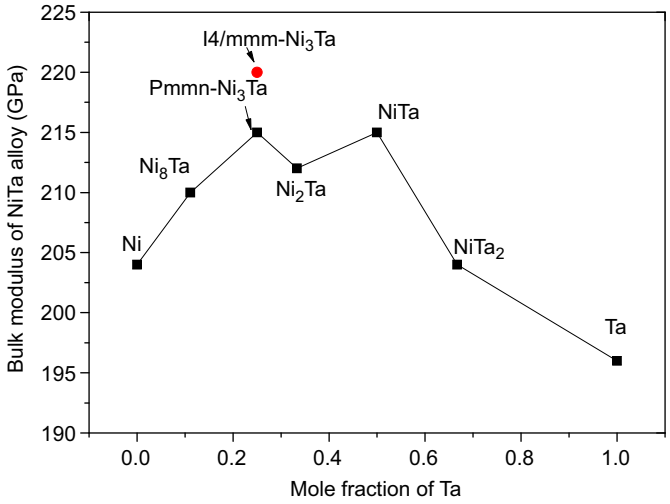


**Fig. 3.** Calculated bulk modulus of Ni–Ta intermetallic compounds.

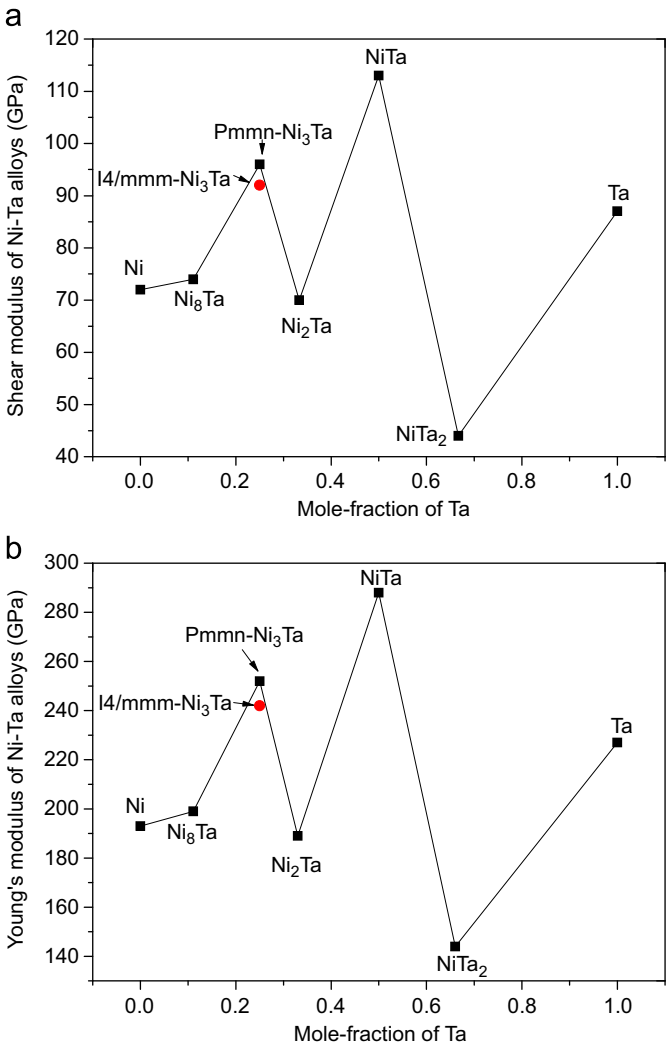


**Fig. 4.** Calculated shear modulus and Young's modulus of Ni–Ta intermetallic compounds.

To make further conclusions on the mechanical properties, polycrystalline bulk modulus ($K$), shear modulus ($G$), Young's modulus ($E$), and Poisson's ratio ($v$) have been calculated by applying the Voigt–Reuss–Hill (VRH) approximation [47,48] for six mechanically stable Ni–Ta intermetallic compounds. For the convenience of the reader they are listed in Table 3. Fig. 3 shows the bulk modulus $K$ with respect to the Ta concentration. As can be seen from Fig. 3, I4/mmm-$Ni_3Ta$ has the highest bulk modulus, with the value of 220 GPa. Fig. 4 shows the Young's modulus $E$ and shear modulus $G$ against the Ta concentration. The variation trend for Young's modulus and shear modulus with Ta concentration are similar. In particular, NiTa has the highest $E$ and $G$ values of 288 GPa and 113 GPa, respectively, whereas the ha-$NiTa_2$ has the lowest $E$ and $G$ values of 144 GPa and 44 GPa, respectively.

In this work, brittleness and ductility properties of Ni–Ta intermetallic compounds have been studied by calculating the ratio of shear modulus to bulk modulus, $G/K$. This can be seen as an empirical criterion of the extent of fracture range in materials. A high value of $G/K$ for a material may be associated with brittleness whereas a low value would correspond to ductility. The critical value that separates brittleness and ductility is around 0.57. That is to say, if $G/K$ value is higher than 0.57 the material behaves in a brittle manner, otherwise the material behaves in a ductile manner [49]. Our calculated $G/K$ values are 0.35, 0.42, 0.45, 0.33, 0.53, and 0.21 for $Ni_8Ta$, I4/mmm-$Ni_3Ta$, Pmmn-$Ni_3Ta$, $Ni_2Ta$, NiTa, and ha-$NiTa_2$, respectively. These results indicate that

**Table 4**
The heats of formation for Ni–Ta intermetallic compounds, calculated in this work known from the literature.

| Compound | Heats of formation (KJ/mol atoms) | Reference |
|---|---|---|
| $Ni_8Ta$ | −15.2026 | This work |
| | −16.37 | [8] CALPHAD |
| I4/mmm-$Ni_3Ta$ | −28.3298 | This work |
| | −35.29 | [8] CALPHAD |
| Pmmn-$Ni_3Ta$ | −29.7379 | This work |
| | −34.81 | [8] CALPHAD |
| $Ni_2Ta$ | −17.8237 | This work |
| | −22.36 | [8] CALPHAD |
| NiTa | −25.6724 | This work |
| | −25.51 | [8] CALPHAD |
| ha-$NiTa_2$ | −17.5287 | This work |
| | −21.75 | [8] CALPHAD |

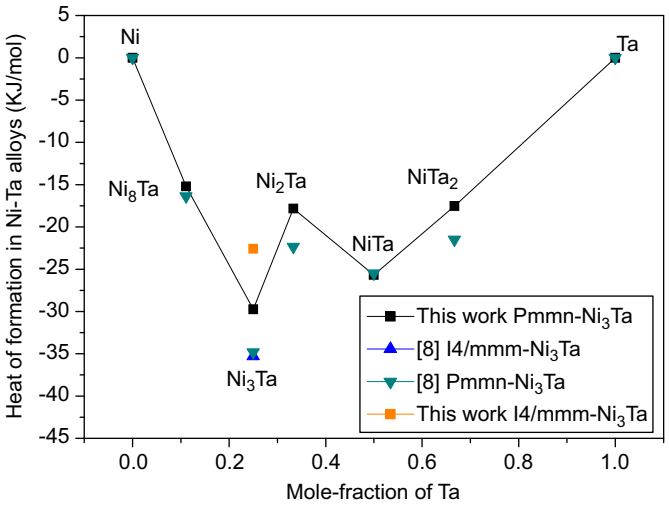


**Fig. 5.** The calculated heats of formation compared to former calculated values for Ni–Ta intermetallic compounds.

six mechanically stable Ni–Ta intermetallic compounds are ductile materials. Poisson's ratio is another characteristic to distinguish the ductility property of materials [50]. Materials with a Poisson's ratio around 1/3 are ductile, while materials with a Poisson's ratio far less than 1/3 are inferred as brittle. Based on our calculated Poisson's ratio, NiTa can be considered as a brittle material, while the other five mechanical stable Ni–Ta intermetallic compounds are ductile materials. We note also that $Ni_3Ta$ has always brittle properties under experimental conditions, and the reason for its brittle properties may be attributed to the precipitates in grain boundaries [9]. Therefore, the single crystal production technology, powder metallurgy, strengthening the grain boundaries, and some other methods are worth a try to ameliorate the intergranular cracking. In this work, the hardness of intermetallics has also been determined based on the corresponding valence electron density. It is known that the high valence electron density signifies high hardness [51]. Our calculated valence electron densities are 0.193, 0.224, 0.212, 0.227, 0.242, 0.256 electron/Å$^3$ for $Ni_8Ta$, I4/mmm-$Ni_3Ta$, Pmmn-$Ni_3Ta$, $Ni_2Ta$, NiTa, $NiTa_2$, respectively. These results show that the hardness increases with the Ta concentration.

### 3.3. Thermodynamic stability and heats of formation

To study the thermodynamic properties, total energies of six mechanical stable Ni–Ta intermetallic compounds and the pure Ni, Ta have been obtained by DFT calculations. Then the heats of formation for Ni–Ta intermetallic compounds can be calculated on the basis of the following formula:

$$E_{\text{form}}^{\text{Ni}_m\text{Ta}_n} = (E_{\text{total}}^{\text{Ni}_m\text{Ta}_n} - mE_{\text{solid}}^{\text{Ni}} - nE_{\text{solid}}^{\text{Ta}})/(m+n) \quad (5)$$

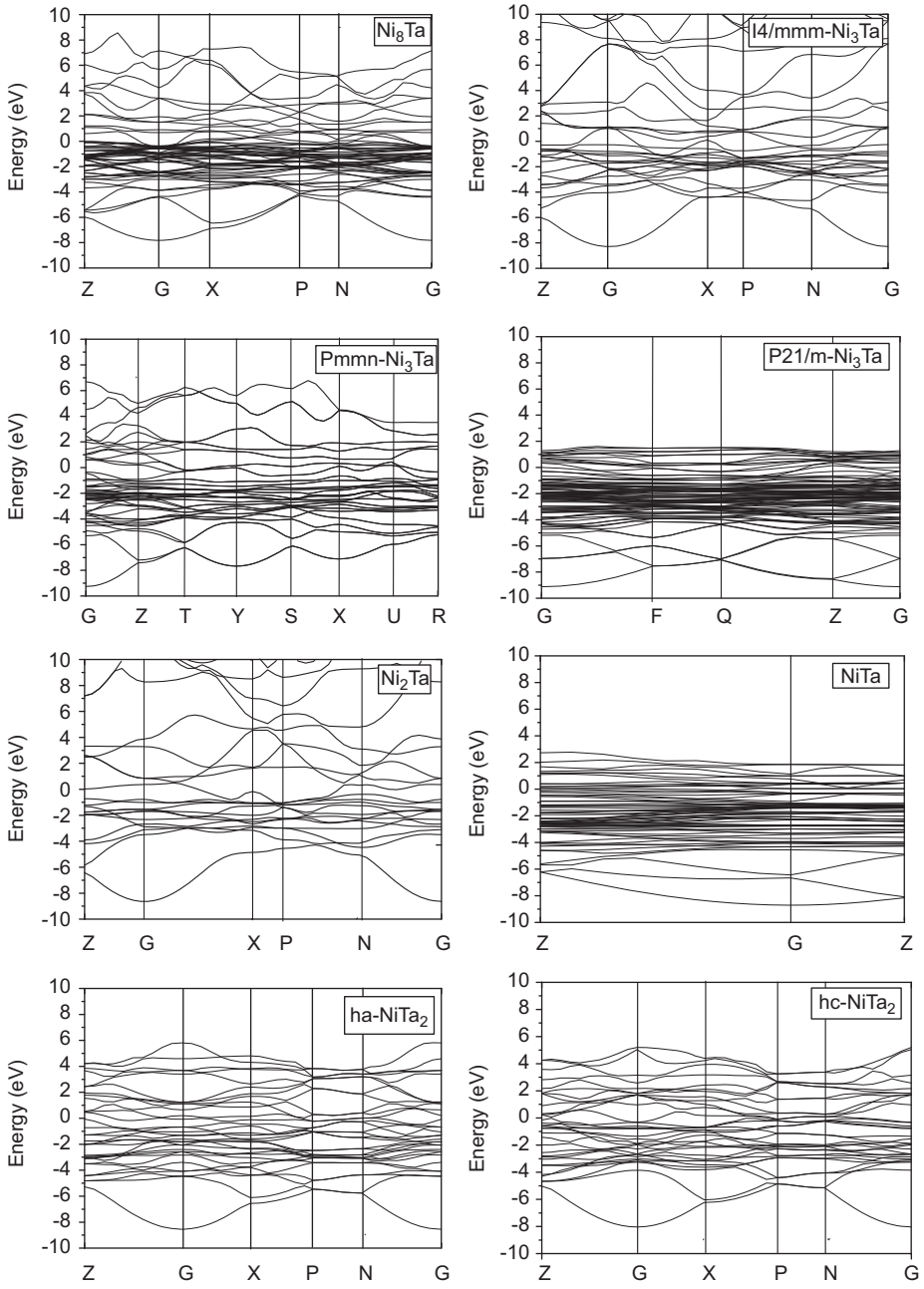


**Fig. 6.** Electronic energy bandstructures of Ni–Ta intermetallic compounds.

where $E_{form}^{Ni_mTa_n}$ is the atomic heats of formation for a $Ni_mTa_n$ alloy, $E_{total}^{Ni_mTa_n}$ refers to the total energy of a $Ni_mTa_n$ primitive cell that includes $m$ Ni atoms and $n$ Ta atoms with equilibrium lattice parameters, $E_{solid}^{Ni}$ is the total energy of a Ni atom with FCC structure, $E_{solid}^{Ta}$ is the total energy of a Ta atom with BCC structure.

Using the formula (5), the heats of formation for mechanically stable Ni–Ta intermetallic compounds have been calculated, and the results are summarized in Table 4 along with the previously known theoretical results found in the literature [8]. It can be seen that the calculated values are in a good agreement with such results. This comparison is also visualized by Fig. 5. As seen in Fig. 5, all the heats of formation are negative, and the absolute values of heats of formation for $Ni_8Ta$, I4/mmm-$Ni_3Ta$, Pmmn-$Ni_3Ta$, P21/m-$Ni_3Ta$, $Ni_2Ta$, NiTa, and ha-$NiTa_2$ are 15.2, 22.6, 29.7, 17.8, 25.7, 17.5 kJ/mol atoms, respectively. These observations imply that the chemical interaction between Ni and Ta is not so tight, but the negative heats of formation ensure that these intermatellic compounds are thermodynamically stable. Nevertheless, $Ni_2Ta$ can be considered as a thermodynamic unstable phase, due to the fact that it can be transformed into lower energy phases of $Ni_3Ta$ and NiTa.

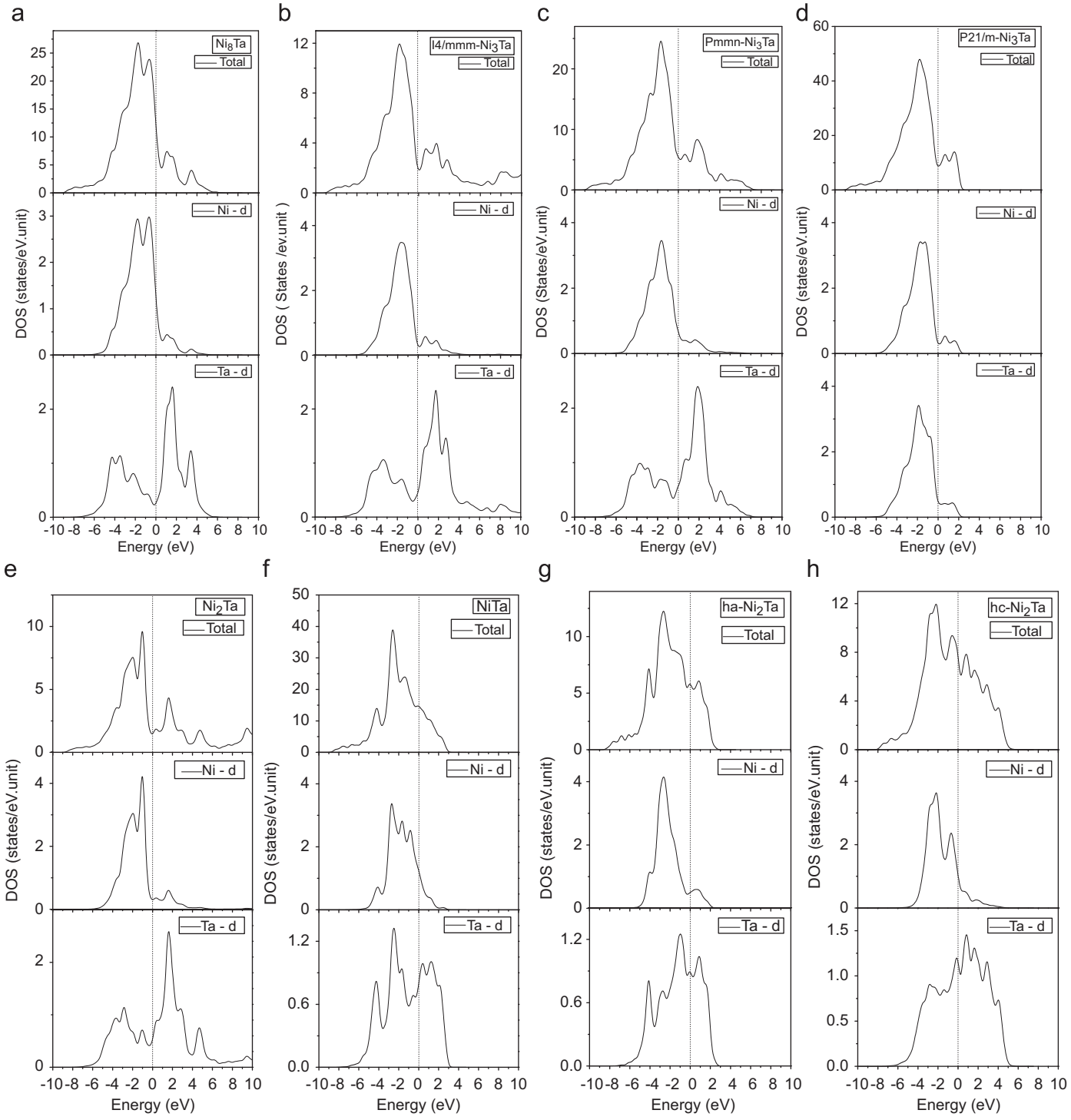


**Fig. 7.** Density of state for Ni–Ta intermetallic compounds.

### 3.4. Electronic energy band structure

In this work, the electronic energy band structures and density of states of the Ni–Ta intermetallic compounds have also been calculated, and they are shown in Figs. 6 and 7, respectively. Electronic energy band structures indicate the energy of point which has symmetry in our intermatallic system. The level at zero energy in Fig. 6 is the Fermi level, which is defined as the highest energy level is occupied by the electrons at 0 K, is located in the band gap. As seen in Fig. 6, the valence band overlaps the conduction band at the Fermi surface. Hence, the Ni–Ta intermetallic compounds considered here are all conducting materials. Besides, as it is indicated clearly in Fig. 7, peaks exist in the two sides of Fermi level. Furthermore, the density of states correspond to the Fermi level was not zero; imply that all the Ni–Ta intermetallics are conductors. According to the partial density of states, the main valence electron contributions of the bonding electrons in the whole regions are Ni(3d) and Ta(5d). Ta-d state and Ni-d state are hybridized in the valence band of these intermetallic compounds except $Ni_2Ta$, the valence band of which is occupied by Ni-d state. Moreover, the bond peaks above Fermi level are conduction band, which are mainly dominated by Ta-d valence electrons for I4/mmm-$Ni_3Ta$, Pmmn-$Ni_3Ta$, $Ni_2Ta$, ha-$NiTa_2$ and hc-$NiTa_2$, while that of NiTa and $Ni_8Ta$ are occupied by Ni-d state. For I4/mmm-$Ni_3Ta$, the Ni-d state and Ta-d state have a hybridization in conduction band. In addition, the distance of the nearest peaks located separately in the two sides of zero energy symbolized the bands, with the increasing of distance, the bond transformed from metallic to covalent. These peaks are close to each other in Fig. 7, which demonstrate the metallicity of these intermetallic compounds. With the increasing of width, the pseudogap for these intermetallics can be sequenced in the order of ha-$NiTa_2$, $Ni_2Ta$, hc-$NiTa_2$, $Ni_8Ta$, P21/m-$Ni_3Ta$, I4/mmm-$Ni_3Ta$, Pmmn-$Ni_3Ta$ and NiTa. The ductility of intermatallics may become weaker as the metallicity of bond reducing, consequently, NiTa has the weakest ductility among these alloys, while ha-$NiTa_2$ has the best ductility, the deformation ability of intermatallics enhanced with the increasing of pseudogap width. This trend is in accordance with the ductility testified by $G/K$ and poisson's ratio values discussed above. As seen in Fig. 7, it is found that the bonding electron numbers per atom below the Fermi level are 9.53, 8.90, 8.87, 8.86, 8.45, 7.82, 6.80, 6.71 for $Ni_8Ta$, I4/mmm-$Ni_3Ta$, P21/m-$Ni_3Ta$, Pmmn-$Ni_3Ta$, $Ni_2Ta$, NiTa, ha-$NiTa_2$, hc-$NiTa_2$, respectively. The larger number of bonding electron, the stronger charge interaction [52,53], and the structural stability of alloy will be better. Thus, the structure stability increases with the Ta concentration.

## 4. Conclusions

In conclusion, we have investigated the structural properties, elastic properties, heats of formation and electronic structures for five Ni–Ta binary intermetallic compounds by utilizing DFT calculations. Our optimized lattice parameters agree well with available experimental values. The mass density of Ni–Ta intermetallic compounds increases approximately in a linear manner with the increasing Ta concentration. All the Ni–Ta intermetallic compounds considered here are mechanically stable, except for P21/m-$Ni_3Ta$ and hc-$NiTa_2$. The polycrystalline elastic modulus and Poisson's ratio have been deduced by the VRH approximation, and the calculated $G/K$ values indicated that $Ni_8Ta$, I4/mmm-$Ni_3Ta$, Pmmn-$Ni_3Ta$, $Ni_2Ta$, NiTa, ha-$NiTa_2$ are ductile materials. The calculated heats of formation for Ni–Ta intermetallic compounds demonstrate that $Ni_2Ta$ is a thermodynamic unstable phase. Our results have also indicated that Pmmn-$Ni_3Ta$ is the ground stable phase of $Ni_3Ta$ polymorphs. The energy band structures calculated in this work demonstrate that all five Ni–Ta intermetallic compounds are conductors. The ductility of Ni–Ta intermetallic compounds deduced from the density of state corresponds very well with the result derived from the $G/K$ and poisson's ratio. The structure stability increases with the Ta concentration.

## Acknowledgments

This work was supported by the National Natural Science Foundation of China (Grant No.'s 51131002, 50772018) and the Program for New Century Excellent Talents in Universities of China (NCET-07–0139). R. M. acknowledges the support from the NSERC and CRC programs.

## References

[1] X.M. Pan, Z.P. Jin, Trans. Nonfer. Met. Soc. China 12 (2002) 748–753.
[2] P.Y. Lee, J.L. Yang, C.K. Lin, H.M. Lin, Metall Mater Trans A 28 (1997) 1429–1435.
[3] E. Therkelsen, Met. Alloys 4 (1933) 105–108.
[4] A. Nash, P. Nash, Bull. Alloy Phase Diagrams 5 (1984) 259–265.
[5] L. Kaufman, CALPHAD 15 (1991) 243–259.
[6] I. Ansara, M. Selleby, CALPHAD 18 (1994) 99–107.
[7] Y.W. Cui, Z.P. Jin, Z. Metallkd. 90 (1999) 233–241.
[8] S.H. Zhou, Y. Wang, L.Q. Chen, Z.K. Liu, R.E. Napolitano, CALPHAD 33 (2009) 631–641.
[9] G.S. Firstov, Y.N. Koval, J. Van Humbeeck, P. Ochin, Mater. Sci. Eng., A 481–482 (2008) 590–593.
[10] A. Rudajevova, J. Pospisil, Mater. Sci. Eng., A 527 (2010) 2900–2905.
[11] N. Karlsson, Jpn. Inst. Met. 79 (1951) 391–405.
[12] H.H. Stadelmaier, Metal. Technol. 18 (1964) 1038–1039.
[13] R.C. Rurl, B.C. Giessen, M. Cohen, N.J. Grant, J. Less-Common Met. 13 (1967) 611–618.
[14] B.C. Giessen, N.J. Grant, Acta Meter. 15 (1967) 871–877.
[15] T. Saburi, M. Nakamura, S. Nenno, J. Less-Common Met. 41 (1975) 135–139.
[16] H.J. Wallbaum, Arch. Eisenhuttenwes 31 (1943) 91–92.
[17] E.E. Havinga, H. Damsma, P. Hokkeling, J. Less-Common Met. 27 (1972) 169–186.
[18] P.I. Kripyakevich, E.N. Pylaeva, J Less-Common Met. 27 (1972) 169–186.
[19] M.D. Segall., P.J.D. Lindan., M.J. Probert, C.J. Pickard, P.J. Hasnip, S.J. Clark, J. Phys.: Condens. Matter 14 (2002) 2717.
[20] D.R. Hamann, M. Schluter, C. Chiang, Phys. Rev. Lett. 43 (1979) 1494.
[21] M.C. Payne, M.P. Teter, D.C. Allan, T.A. Arias, J.D. Joannopoulos, Rev. Mod. Phys. 64 (1992) 1045.
[22] J.P. Perdew, K. Burke, M. Ernzerhof, Phys. Rev. Lett. 77 (1996) 3865.
[23] H.Y. Geng, N.X. Chen, M.H.F. Sluiter, Phys. Rev. B 70 (2004) 094203; Diagrams Thermochem. 33 (2009) 631–641.
[24] P.I. Kripyakevich, E.N. Pylaeva, Kristallografiya 12 (1967) 350–352.
[25] B.C. Giessen, N.J. Grant, Trans Metall. Soc. Aime 230 (1964) 1730–1731.
[26] A. Magneli, A. Westgren, Z. Anorg. Allg. Chem. 238 (1938) 268–272.
[27] H. Arnfelt, A. Westgren, Jernkontorets Ann. 119 (1935) 185–196.
[28] P. Pietrokowsky, Nature (London) 206 (1965). 291-291.
[29] P.I. Kripyakevich, E.I. Gladyshevskii, E.N. Pylaeva, Kristallografiya 7 (2) (1962) 212–216.
[30] J.T. Zhao, L. Gelato, E. Parthe, Acta Crystallogr., C 47 (1991) 479–483.
[31] H. Nowotny, H. Oesterreicher, Monatsh. Chem. 95 (1964) 982–989.
[32] E.N. Pylaeva, E.I. Gladyshevskii, P.I. Kripyakevich, Zh. Neorg. Khim. 3 (1958) 1626–1631.
[33] R.H. Taylor, S. Curtarolo, L.W. Hart, J. Am. Chem. Soc.
[34] J.M. Larson, R. Taggart, D.H. Polonis, Metall. Trans. 1 (1970) 485–489.
[35] M.P. Arbuzov, V.G. Chuprina, Poroshk. Metall. 2 (1978) 72–75.
[36] V.S. Kogan, A.S. Bulatov, Zh. Eksp. Teor. Fiz. 42 (1962) 1499–1501.
[37] E.A. Owen, E.L. Yates, Philos. Mag. 21 (1936) 809–819.
[38] E.R. Jette, F. Foote, J. Chem. Phys. 3 (1935) 605–616.
[39] G. Brauer, K.H. Zapp, Z. Anorg. Allg. Chem. 277 (1954) 129–139.
[40] H.E. Swanson, E. Tatge, National Bureau of Standards (U.S.), Circular 539 (1953) 1–95.
[41] J.W. Edwards, R. Speiser, H.L. Johnston, J. Appl. Phys. 22 (1951) 424–428.
[42] X.L. Wang, F.B. Tian, L.C. Wang, T. Cui, B.B. Liu, G.T. Zou, J. Chem. Phys. 132 (2010) 024502.
[43] D.C. Wallace, Thermodynamics of Crystal, Wiley, New York, 1972. Chapter 1.
[44] X.Y. Huang, I.I. Naumov, K.M. Rabe, Phys. Rev. B 70 (2004) 064301.
[45] Y.L. Amy, R.M. Wentzcovitch, Phys. Rev. B 50 (1994) 10632.
[46] B.B. Karki, G. Ackland, J. Crian, J. Phys.: Condens. Matter 9 (1997) 8579.
[47] O.L. Anderson, J. Phys. Chem. Solids 24 (1963) 909.
[48] J. Haines, J.M. Leger, G. Bocquillon, Annu. Rev. Mater. Res. 31 (2001) 1.

[49] S.F. Pugh, Philos. Mag. 45 (1954) 823.
[50] I.N. Frantsevich, F.F. Voronov, S.A. Bokuta, Elastic Constants and Elastic Moduli of Metals and Insulators Handbook, in: I.N. Frantsevich (Ed.), Naukova Dumka, Kiev, 1983, pp. 60–180.
[51] L. Pauling., The Nature of Chemical Bond, Cornell University Press, Cornell, 1960.
[52] C. Fu, X. Wang, Y. Ye, K. Ho, Intermetallics 7 (1999) 179–184.
[53] J. Nylen, F.J. Garcia Garcia, B.D. Mosel, R. Pottgen, U. Haussermann, Solid State Sci. 6 (2004) 147–155.